WHEEL RAIL CONTACT DAMAGE FROM HIGH ADHESION LOCOMOTIVES, AND DAMAGE MITIGATION FROM STEERING BOGIES

Scott Simson[1], Colin Cole[1]

Phd, ME, Grad Dip IT, BE Prof, Phd, ME, BE

1. Centre for Railway Engineering, CQUniversity, Australia

SUMMARY

The development of improved traction control and adoption of AC traction motors has led to the development of high adhesion locomotives. Rollingstock manufacturers have been successful in marketing these high adhesion locomotives to train operators because of the increase in continuous tractive effort these locomotives provide allowing larger trains to be hauled over ruling grades. Some concerns have been held by track infrastructure owners in the Australian rail industry about the rail damage associated with high adhesion locomotives in operation on the tight curves associated with ruling grades. This paper uses vehicle dynamics simulation to determine the wheel rail contact forces of high adhesion locomotive operations on steep grades (up to 1 in 37) and compares the advantages to be gained from the use of distributed power and steering bogie designs to current locomotives and head end trains. The reduction of the available adhesion due to wheelset angle of attack is demonstrated by the simulation.

INTRODUCTION

The development of high adhesion AC traction motors for the rail industry has allowed the locomotives to be operated with much higher continuous traction force and adhesion levels than previously achieved. The operational advantage of this is that train consists which had previously required smaller trailing loads in order to traverse the largest ruling grade can now operate with larger loads. There are examples in Australia where this higher adhesion capability could be used with adhesion levels over 0.3 on curves under 250m radius with widened gauge. Such curves produce very high angles of attack under most wheels. The reduced power per trailing tonne in the train consist means the train is travelling slower over the ruling grade leading to conditions of greater cant imbalance on the wheel loads during curving combined with higher string lining coupler loads.

Previous studies [1] have shown that current passive steering bogies under high adhesion demands fail to reduce the wheelset angle of attack. Forced steering bogies provide some improvement and were found in extensive studies in a PhD thesis [2] to give improved traction in curves except under high string lining forces [1,2]. In this same thesis various steering designs with active control systems were also evaluated. The most promising and practical of these more advanced traction bogie designs has been patented by the Centre for Railway Engineering, CQU. This bogie will be referred to as the AY-FS bogie [2,3] and will be used for comparisons in this paper. The results from the AY-FS bogie were impressive in that good steering was retained and it achieved very low wheelset angles of attack even at adhesion saturation [2,3].

NOTATION

a	Contact patch half length
A	ratio static friction to infinite sliding friction
b	contact patch half width
B	reduction factor for the friction coefficient
c	Specific heat
F_z	vertical wheel contact force
$f_1(\varepsilon)$	Non dimensional function between 0–0.538
k	Fatigue stress limit of the rail steel
N	Normal contact force
p_o	Maximum contact pressure
s_r	Slip rate or creepage
s_x	Longitudinal slip rate or creepage
T	Traction contact force
v_o	velocity
λ	Thermal conductivity
ρ	density
μ	Friction coefficient
μ_x	Traction or longitudinal friction, coefficient
μ_0	Friction coefficient at zero slip

TRAIN TEST ON THE PROPOSED TRAINS

There is a proposed train operation on the North South route using three high adhesion 134 tonne locomotives with 4500 trailing tonnes. The most constraining location is on the Cowan Bank on RailCorp track North of Sydney. Cowan Bank has an extended section with grades of 1 in 40 and curves of 220 m radius. The track grades and curves for Cowan Bank are shown in Figure 1.

For the purposes of assessing the proposed operation, all weather adhesion train tests were performed by using water sprays on the leading locomotive [4]. The all weather test has been passed by trains operating with high adhesion locomotives supplied from both EDI Rail and United Group.

Energy and Force Calculation

In an energy calculation based on the SCT class locomotive [5] and using the Davis equation [6] for rolling resistances, the 6 km track section to Boronia requires 2456 MJ per locomotive. That is 11 times initial kinetic energy of the train travelling at speed in the 60 km/h speed limit section across the Hawksbury River. The energy needs requires 14:15 mins of full power and hence an average speed of 25.3 km/h. The peak force demand to equalise the rolling and grade resistance is dependant on the train length as a small section ~250 m of the track has a steeper grade of 1:37 below the 54 km post and peak forces occur soon after.

Longitudinal Train Simulations

The train forces and speeds required with the consists of: triple head 4500 trailing tonne and double head 3000 trailing tonne trains were confirmed using simulation. Train simulations were completed using the longitudinal train simulator developed at the Centre for Railway Engineering, CRE-LTS. The trains were modelled with a typical high adhesion locomotive model , with a peak traction performance of 630 kN and traction power of 2862 kW. While there is no intentional bias toward locomotive suppliers and the same locomotive model was used for all simulations, it will be realized that the specification approximates to the various versions of the EDI GT46C. The modelling used has field validation in general operations via its usage in the intelligent train monitor on the QR 4000 class locomotives [7]. The Centre did not have similar validated modelling available for the UGL C44aci at the time of writing this paper so only the one model was used. (So, the paper cannot be used to fuel locomotive supplier debates).

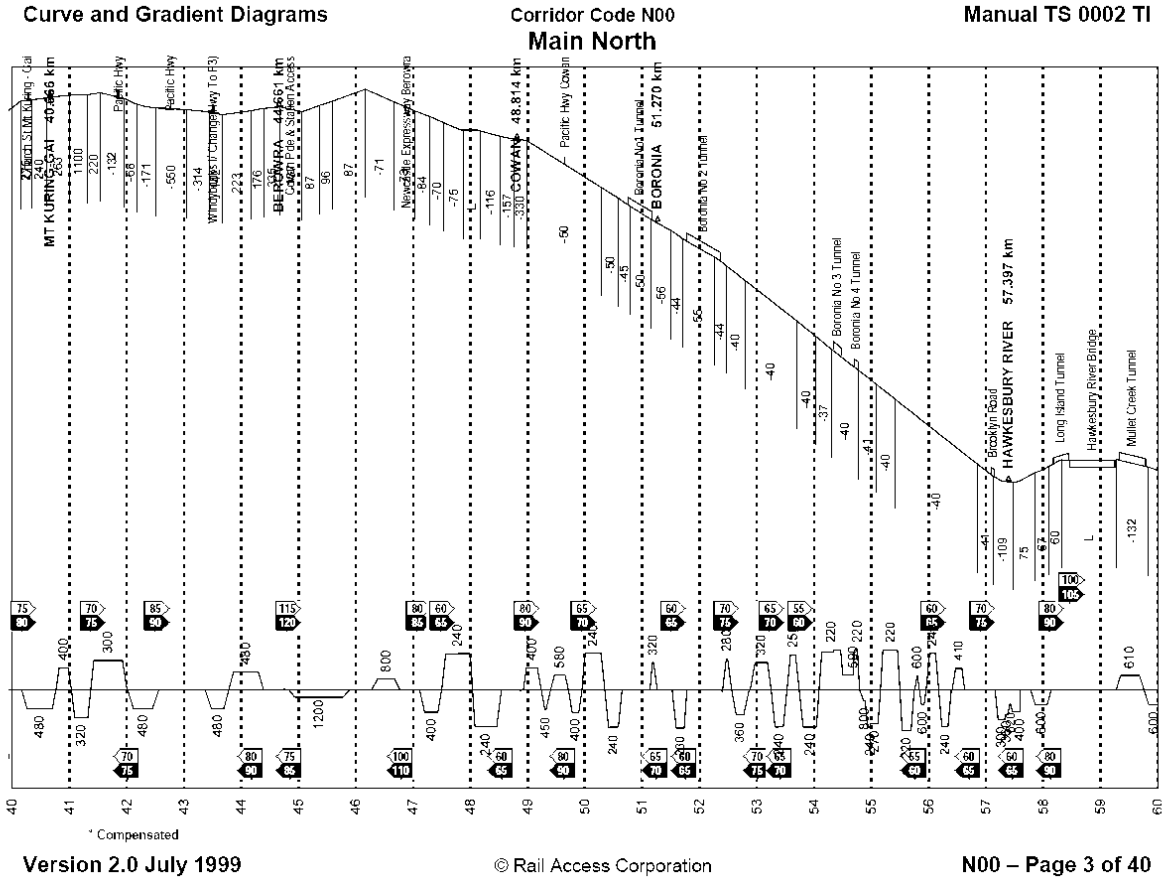

Figure 1 Cowan Bank

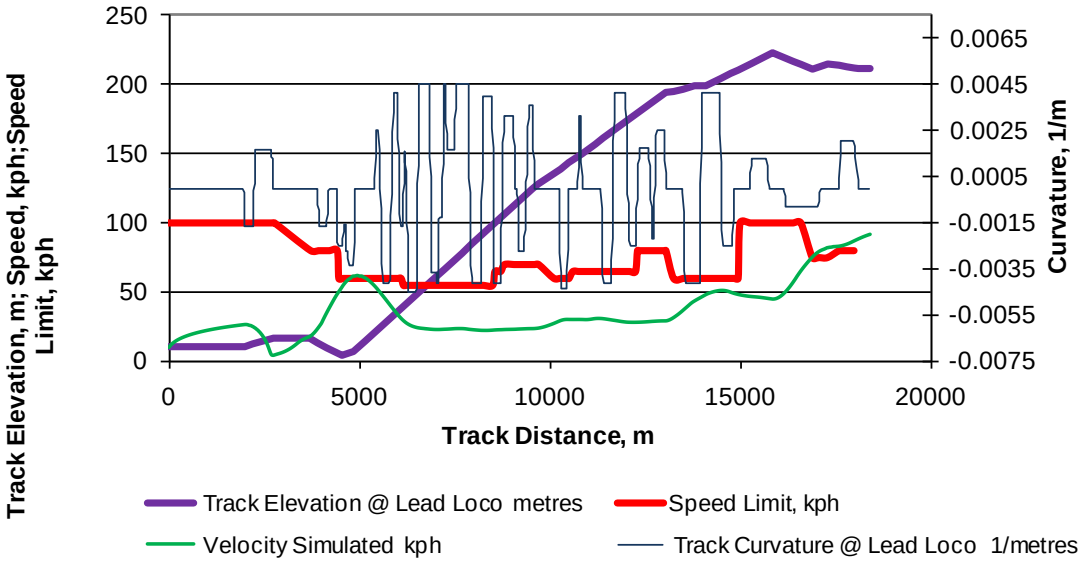

Figure 2 Track topography, curvatures, simulated speed and track speed limits

The train was modelled in the usual way with non-linear draft gear connections, wagons were taken as 100 tonne gross giving 30 and 45 wagon trains respectively for the two cases. The wagon length over coupler faces was set at 20m. Rolling and air resistance was modelled with the modified Davis equation [6] and the curving resistance was modelled using the approximate 6116/R N/tonne (where R is the curve radius in m.) [6].

The trains were simulated on the Cowan Bank track topography with driving strategies kept as simple as possible. Particular care was taken in the selection of throttle levels to ensure the locomotives were set at full power before the climb to ensure that in-train force transients did not add to the high drawbar forces required. The driving strategy was also made compliant with the required speed limits. The track topography and operational data is shown above in Figure 2.

Train Simulation Results:

The simulation results are shown in Figure 3 and Figure 4. There are only minor differences in speed profile and individual locomotive performances of the two trains. The longer train, of course, uses potential energy slightly better, the minimum speed of the heavier longer train was very slightly higher than the lighter train, 22.4km/h verses 22.2 km/h.

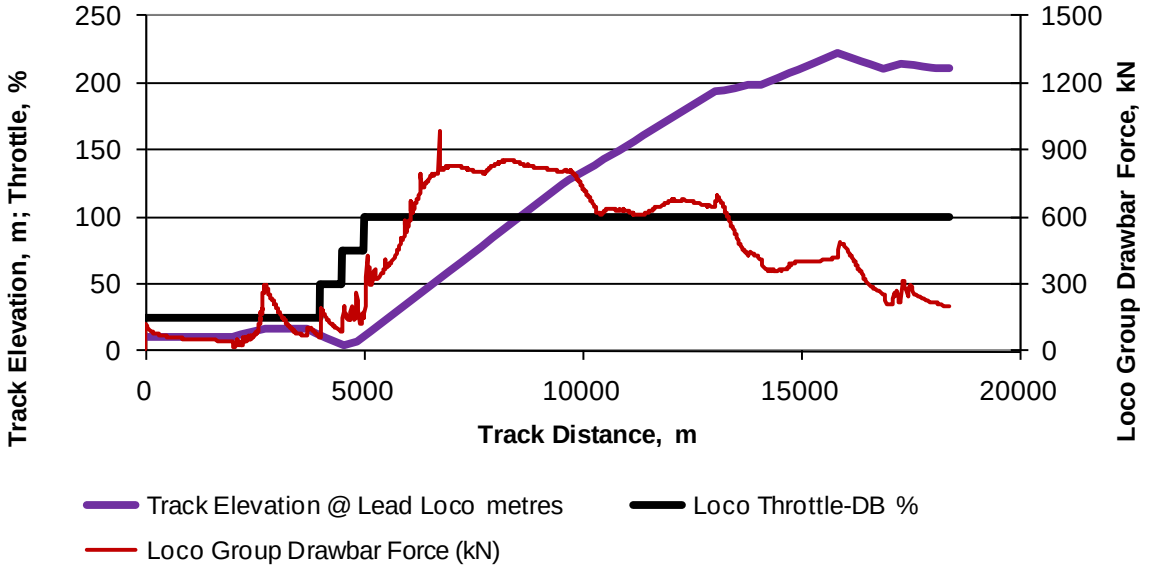

Figure 3 Train Simulation – 3000 tonne Train

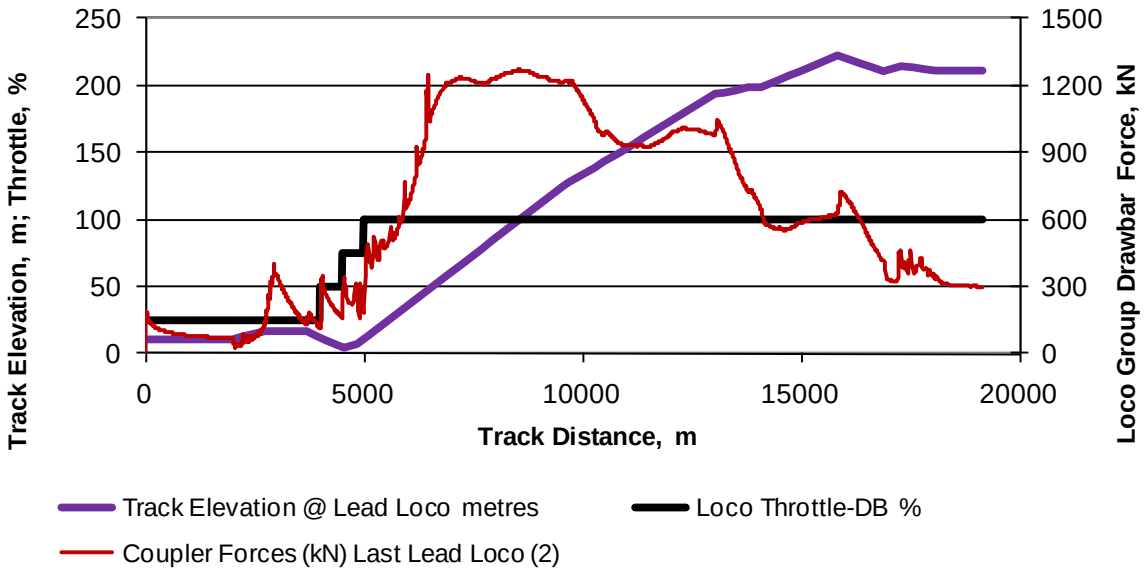

Figure 4 Train Simulation – 4500 tonne Train

In-train force peaks which include transients were 984kN (3000t train), and 1272kN (4500t train), Figure 3 and Figure 4, but steady traction forces going into the system are 463.2kN per loco (926.4kN total) and 459.1 kN per loco (1377.3kN total) respectively. The discrepancy between the traction inputs and in-train forces is due to differences in transient accelerations and grade forces on the locomotives at the instances in time when the maximums occurred.

Results for Vehicle Simulation

To replicate the train test in vehicle simulation a test of constant speed of 22.4 km/h at adhesion of 0.350 which equates to a 460 kN tractive force was run using track geometry from 55.1 – 52.3 km. Coupler forces on the vehicle were modelled for the coupler height of 0.83 m using coupler angle calculations to give lateral and yaw loads. For a constant 220m radius curve the lateral coupler load and yaw loads and the total expected lateral load are shown in Table 1.

CONTACT PATCH FORCES

Surface initiated rolling contact fatigue (RCF) stresses increase with wheel rail creep forces, [11]. When the creep force coefficient level reaches a level of approximately 0.3 of the normal force the maximum shear stress in the wheel rail contact coincides with the surface as opposed to being at a contact patch radius depth below the surface. This then makes surface initiated RCF cracks such as head checks and rail squats more prevalent. The adhesion demand on the Cowan Bank test of 0.350 is sufficient to cause RCF initiation in tangent track. Surface initiated fatigue indexes can be calculated using Equation 1. These are sensitive to maximum contact stress.

Locomotive	Coupler Lateral [KN]	Coupler Yaw [KN.m]	Total Lateral [KN]
Single	31	308	-76
Double	83	404	-128
Triple	135	501	-180

Table 1 Lateral coupler loads based on 0.350 adhesion, 220 m radius curve, 22.4 km/h, 82 mm cant

$$FL_{surf} = \mu - \frac{2\pi \cdot a \cdot b \cdot k}{3F_z}$$

Equation 1 - Surface fatigue limit stresses [8]

Under traction the contact fatigue stresses experienced by the rail have been shown to be greater than at the wheel or rail at any other time, [9]. This is because thermal stresses for the rail in traction add to the maximum shear stresses in the contact patch. The theoretic change in the shake down map for an extreme case is given Figure 5. Figure 5 is for a constant thermal stress but in practise the thermal stress changes with traction coefficient

Temperature Effects at High Wheel Slip Rates

At high levels of contact stress and slip rate the thermal energy into the wheel rail contact softens the surfaces reducing the effective friction coefficient, [10]. The flash temperature of the wheel rail contacts increase with contact pressure and slip rate, (creepage times velocity). Assuming the wheel rail contact is in full slip the equation for

contact flash temperature is given in Equation 2, [11] where the variables are friction coefficient, slip rate, contact pressure, contact patch half ellipse length and train velocity.

$$T_r = \frac{\pi \cdot \mu \cdot s_r \cdot p_o}{(2 - s_r) \cdot 4} \cdot \sqrt{\frac{2 \cdot a \cdot v_o}{\lambda \cdot \rho \cdot c}} \cdot f_1(\varepsilon)$$

Equation 2 - Temperature rise in the rail [11]

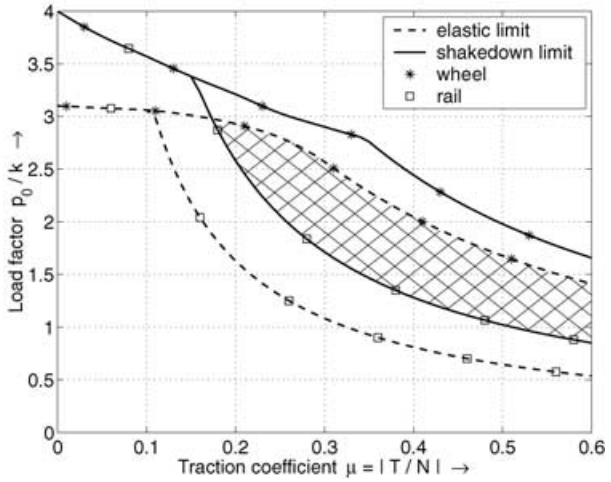

Figure 5 Shackdown map showing temperature effects on the wheel and rail in traction [9]

Temperature is identified as the main cause of the reduction in creep force coefficient past the point of saturation and also the cause for the reduction in creep coefficients seen at high speeds in high speed trains [12,]. Polach [12] has proposed a model for reducing the friction coefficient after saturation for using in vehicle dynamic modelling. Equation 3 shows the friction reduction equation.

$$\mu = \mu_0 \times \left((1 - A) \times e^{-B \cdot s_r \cdot v_0} + A \right)$$

Equation 3 - Friction coefficient reduction [12]

The contact patch flash temperature changes the material properties of the steel and in extreme cases cause changes to the material crystal structure. The material strength, hardness and elastic modulus all reduce with temperature and are causal to the reduction in friction coefficients [10], effecting fatigue and wear resistance. However it is important to understand the rail and wheel surfaces are not perfectly smooth and that asperities on the surface experience much higher contact stresses and flash temperatures than the patch in general increasing wear rates above fatigue.

Measurements of wet sand adhesion exhibits a higher reduction in adhesion than other surfaces, example data is shown in Figure 6. The reason for this is likely to be that contact flash temperatures become concentrated on the sand particles. Actual creep coefficient measurement curves for wheel rail contacts such as Figure 6 are uncommon. Most creep testing is done with scaled test rigs which do not match the required contact patch length *a* or velocity v_0 that are important to the contact flash temperature (Equation 2). The results in Figure 6 can not be used for this simulation as the graph refers only to friction levels much lower than 0.35.

Polach's parameters used in the study are: μ_0 = 0.46; A = 0.4; B = 1.2 for the top of rail contacts; of μ_0 = 0.27; A = 0.4; B = 0.2 for the gauge face contacts. The later is typical of a wet rail values as shown in Figure 6 but is used here to reflect sanding application avoiding the gauge corner area. Creep force coefficients for a well lubricated gauge face could be considerably lower as per the soap solution result shown in Figure 6. Figure 7 shows the creep coefficient creepage curves for the top of rail and gauge face parameters with dry rail parameters.

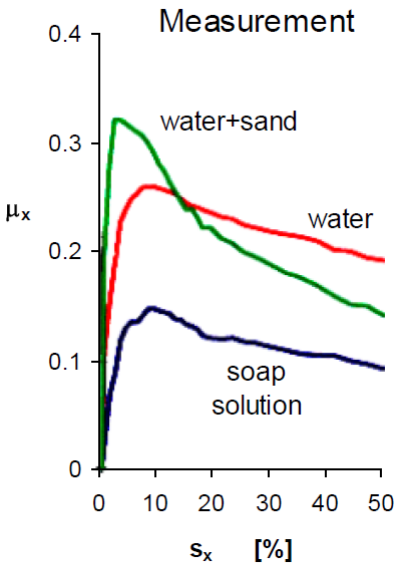

Figure 6 Adhesion tests with a SBB 460 locomotive at 20 km/h [12]

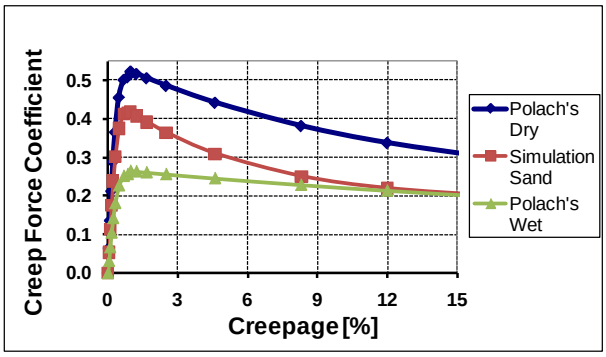

Figure 7 Creep coefficient creepage curves for 22.4 km/h

The choice of creep coefficient parameters is highly significant to the simulation results. A higher creep coefficient curve with a small reduction in the negative part of the curve will reduce the risk

of a wheel slip occurring under any given traction control.

Adhesion Curve for Angle of Attack

Contact creep forces are generated in planar friction, the maximum creep force occurs in the direction of maximum creepage which is a vector sum between longitudinal, lateral creeps. Creep saturation typically occurs at a creepage of 1% or with an angle of attack of 10 mrad. As a result, the angle of attack of the wheelset changes the longitudinal creep or adhesion curve. At high creepages the friction coefficient between wheels and rails is reduced by temperature increases near the surfaces. The temperature rise (Equation 2) is primarily affected by the slip rate, friction coefficient and the velocity. Contact pressure and patch length also has a large influence to gauge corner contact flash temperatures.

The typical influence of the wheelset angle of attack on the adhesion creepage curve is displayed in Figure 8 using the selected study curve. The zero angle curve is further influenced by speed and surface roughness as reported by Polach [12] as well as third body contamination or lubrication [10]. However Polach's results where maximum creep coefficient is much greater than 1% slip from surface roughness and lubricants have not been replicated in scaled test rigs or in Tomberger's model [10].

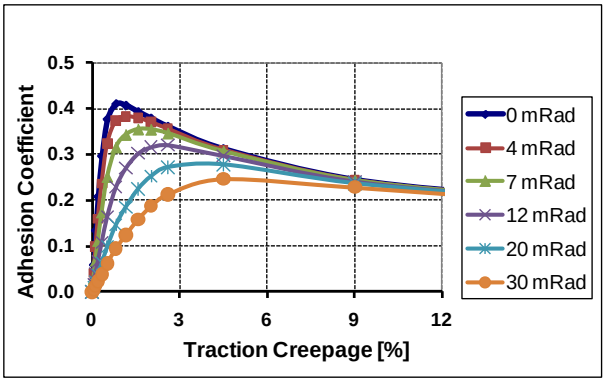

Figure 8 Adhesion Creepage Curves

The simulation at 22.4 km/h on the chosen curve gives a maximum effective adhesion of 0.418. However at 22.4 km/h and with a 7 mrad angle of attack the maximum adhesion drops to 0.355. Adhesion is also greatly compromised by flange contact where maximum friction is likely to be less than 0.24. Thus minimising the wheel flange contact forces will be important to maintaining adhesion.

Wheel Loading Imbalance

Vertical wheel forces during traction curving are affected by the traction induced pitching of the locomotive and the bogies as well as the sway moments induced by the combined effects of cant, centrifugal acceleration and lateral coupler force components. The result is a significant increase in the low rail contact force particularly at the trailing axle of the trailing bogie. With a traction force of 460 kN vehicle pitch is expected to be 3.9% of bogie load, bolster pitching of 6.2% of the wheel load. Changes in loading on different wheels will depend on cant, roll and sway. Sway loading, percentage on the low rail will depend on which locomotive in the locomotive group is being analysed. The front locomotive is expected to have 6.8% increase on the low rail whilst the third locomotive is expected to have 15.5% wheel load increase. The difference is due to the lateral components of coupler forces.

The use of distributed power can considerably reduce the lateral coupler loads and wheel loading on the low rail.

VEHICLE DYNAMICS SIMULATION

Simulations have been performed over the critical track section at train speed 22.4 km/h and a tractive effort of 460 KN. The simulation uses track data recording from Railcorp for gauge, cross level, curvature and top, though preliminary results use idealised track geometry. The simulation has been performed with GENSYS. The wheel rail contacts are calculated for each wheel accounting for the track gauge with much of Cowan bank track curves have gauge widths up to 1456 mm. For low or no adhesion curving the gauge widening allows for a greater rolling radius difference between wheels improving steering. For high adhesion curving, and at slow speeds, the large amount of gauge widening will permit the bogie yaw angle to increase and deteriorate steering.

Locomotive Models

Locomotive vehicle models have been made and tested for five types of bogies. Rigid frame (92 Class), yaw relaxation (SCT class), self steer (QR 4000 class), force steered and the CQU patented AY-FS bogie. Force steering bogies use linkages to force the steering angle of the axles to match the yaw angle of the bogie to the vehicle. The AY-FS bogie combines force steering with bogie yaw actuation. Figure 9 depicts the various bogie types modelled in simulation. Previous studies [1, 3] have shown that at high adhesion levels the yaw relax bogies and self steer bogies fail to provide steering. The force steered bogie achieves partial steering reducing wheelset angle of attack. Aside from the bogie suspension differences in these designs the vehicle modelling is identical.

Traction Control

The simulations have been run with the traction control compensating for the expect bogie and vehicle pitching. The traction motor and control dynamics have not been given detailed modelling

in this study. A simple traction control has been made to intervene to reduce traction power when the wheelset slip rate exceeds 7% with power reducing to zero as the slip rate increases to 27%. The traction control response is limited by 15 Hz filtering to reflect the physical limitation of axle pitch flexibility of the wheelsets and motor frequency delaying the control response. This simple traction control model is not adequately refined for the simulations wet sand creep coefficient curve (Figure 7) though would give a reasonable performance for the wet rail creep coefficient curve.

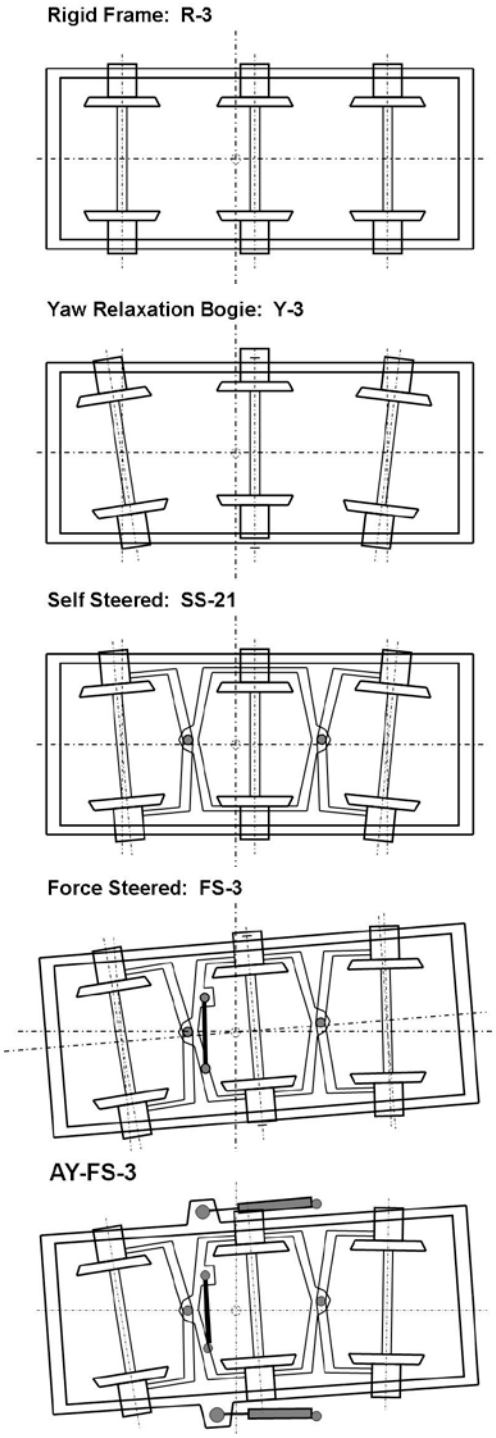

Figure 9 Steering designs of bogies

VEHICLE DYNAMIC RESULTS

The simulation results are reported here are the traction effort of the simulation (Figure 10) and the wheelset angle of attack (Figure 11). The simulations reported here are limited to idealised track for which no traction control instability occurred. The traction control model used resulted in relatively large traction reductions with wheel slip events – this is known to be inferior to existing locomotive systems.

The traction effort Figure 10 indicates if the vehicle is likely to succeed or fail to haul 4500 tonne train. Figure 10 shows results for both a leading locomotive and a third locomotive in a triple head group. With 1500 trailing tones per locomotive a short fall of 16.3 kN below the target of 460kN is a deceleration of 0.1 m/s^2 and is more than sufficient to stop the train. Using ideal track with gauge widening of 16 mm all the bogie types exhibit some loss under the conditions of 0.350 adhesion and 460 KN tractive effort.

Of the passive suspension designs only a lead locomotive with forced steering is able to maintain sufficient tractive effort. Second and third locomotives in a triple head group are out performed by the single lead locomotive. This result confirms the advantages of distributed power in reducing string lining coupler forces.

The rigid frame, yaw relaxation and self steer bogies all fail to steer with the front bogie, bogie yaws of 7 mrad giving the lead axles an angle of attack of 18 mrad (see Figure 11). The force steered bogie has partial steering on the front bogie but due to the wide gauge the lead bogie yaws to 4 mrad this limits the lead axles angle of attack to 8 mrad.

The rear bogies experience much higher lateral curving forces from the coupler loads and are pulled to the low rail. The force steered rear bogie achieves near ideal steering. However, the other bogie designs incur low rail flanging on the middle axle together with angles of attack of unsteered front and rear axles and high rolling radius differences all of which leads to losses in the maximum available adhesion at the rear bogie in the sharper curves. Figure 11 show the angle of attack of the trailing axle on the trailing bogie which is approximately -10 mrad for rigid, yaw relaxation and self steered bogies. The forced steered bogies rear axle angle of attack is between 1-2 mrad for the first locomotive but the third locomotive suffers adhesion loss in the fourth curve with an angle of attack of 6 mrad.

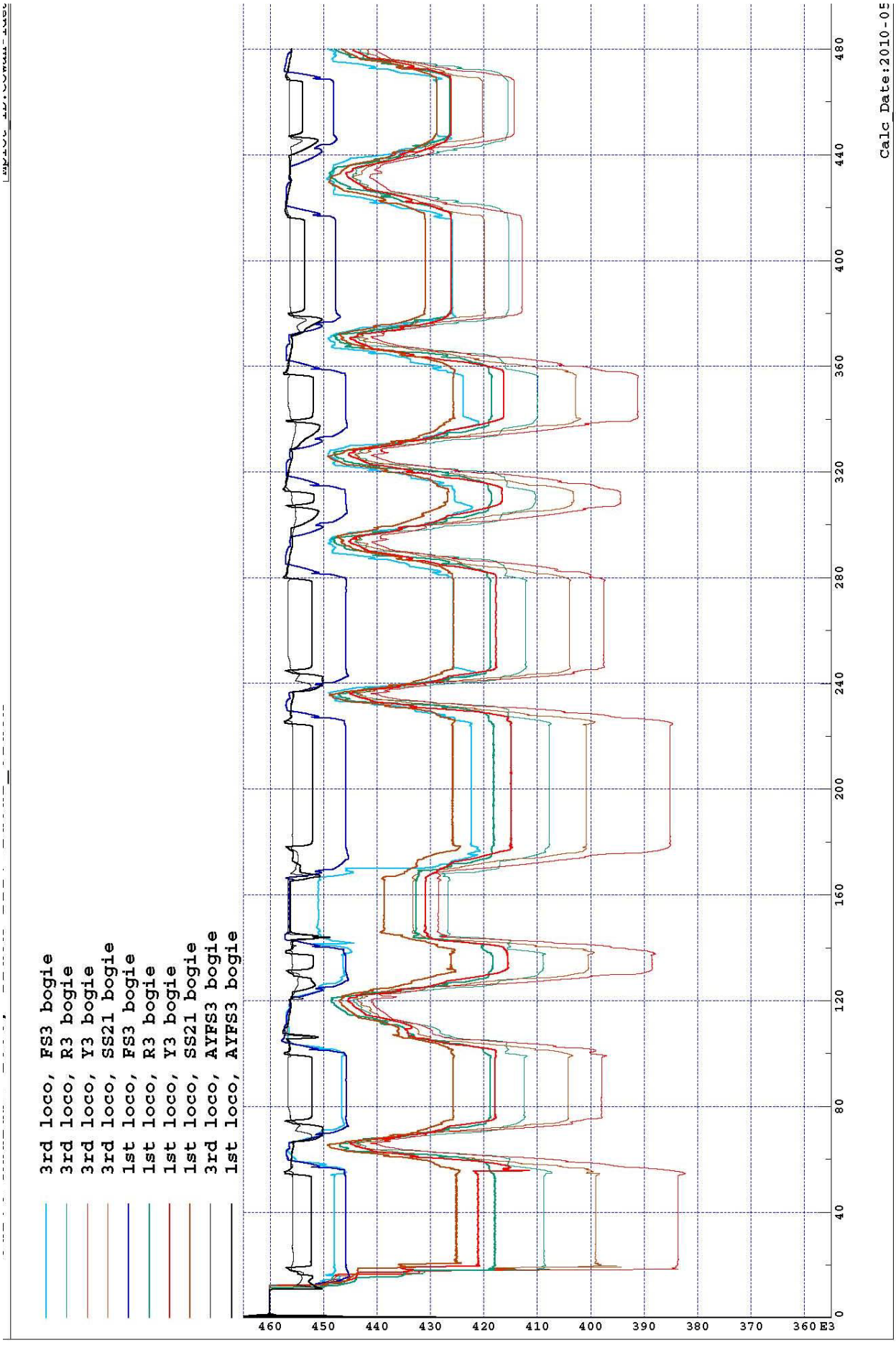

Figure 10 Locomotive traction effort results ideal track

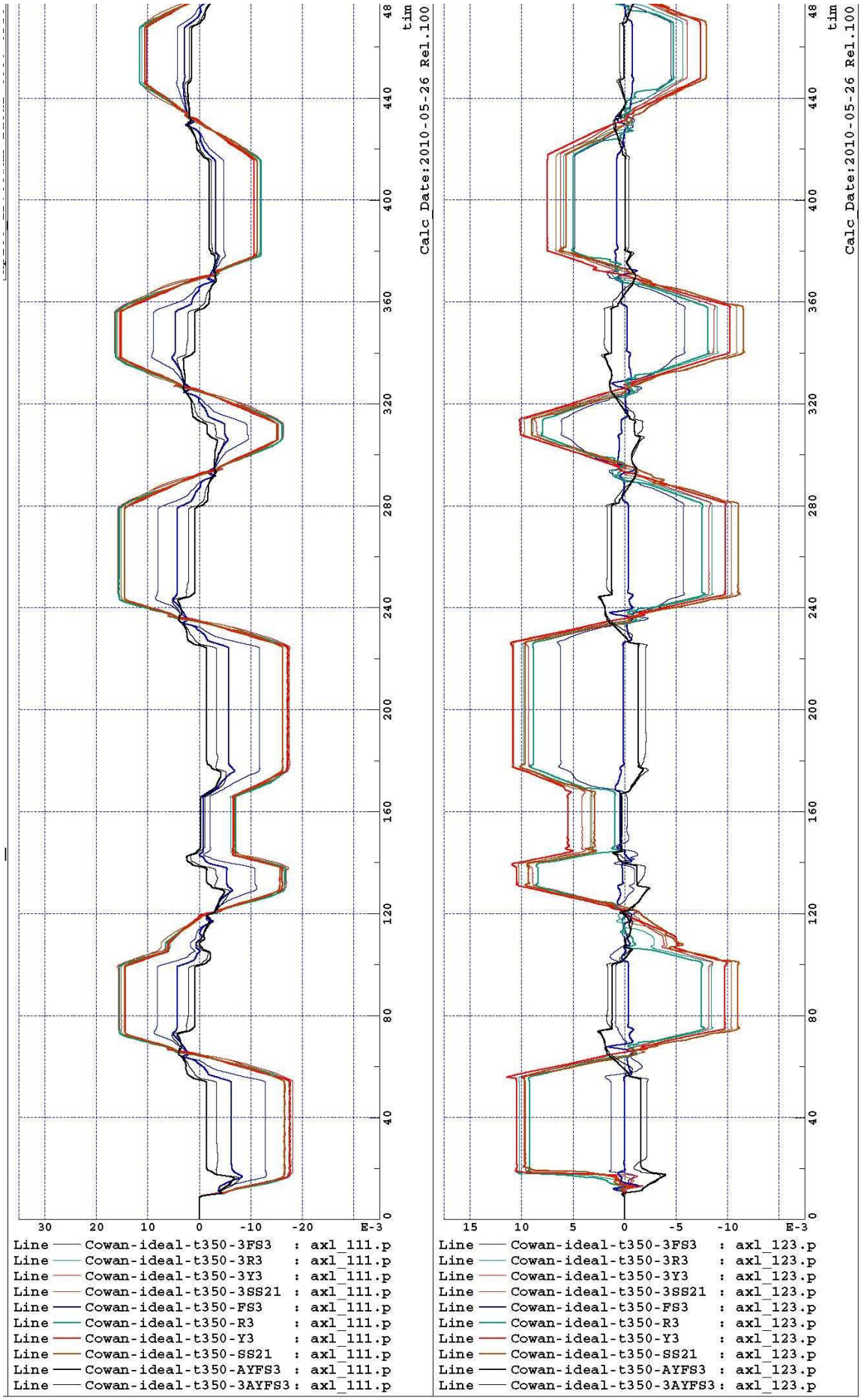

Figure 11 Leading and trailing wheelset angle of attack

The AY-FS bogie design, developed in a research program to concept design stage (patented by CQU), is shown, using the same simulation test method, to be able to maintain steering at all levels of adhesion demand. The wheelset angle of attack in the AY-FS bogie is maintained to under 4 mrad in curve transitions and under 2 mrad in constant curves (Figure 11) with available adhesion thus maintained to 0.385 being well above the traction demand Figure 8.

Current operating EDI and United Group locomotives which are yaw relaxation of rigid bogie designs have passed the all weather testing on Cowan Bank. This shows that the both the traction controls of the locomotives and the creep coefficients from on board sanding has provided better adhesion than modelled in the reported simulation. It also shows that whilst wheelset steering is advantageous to adhesion the most important aspects of adhesion are in the traction control and in sanding equipment to raise friction coefficients.

Rail Damage

Rail damage is modelled based on Burstow's modelling [13] using creep energy Tγ (creep force multiplied by creepage) and Eckberg's modelling. Both rail wear and surface crack growth increase with Tγ though at high levels of Tγ the wear rate can exceed the growth rate of RCF cracks controlling the development of RCF. Burstow's model [13] is empirical and based on lighter axle load passenger rollingstock and lower grade rail steel. Eckberg's model [15] is mechanistic and can be set for head harden rail. Contact patch flash temperatures have also been calculated based on Ertz [11].

Tγ values exceed 200 N on tangent track which according to Burstow is above RCF critical areas and is into high wear regime [14]. However the higher axle loads of Australian freight locomotives compared to UK passenger stock and the averaging used in Burstow's study means the Burstow values should be increased with peak RCF damage at approximately 350 N and wear domination occuring at 500 N. Thus tangent values at 0.350 adhesion are consistent with medium RCF damage. Ekberg's surface fatigue index results, Equation 1 are heavily dependent on contact stresses and thus profiles and tracking positions. Tγ values quickly rise to 600 N in curves with some wheels going into uncontrolled slip and Tγ values over 3000 N. A 600 N Tγ value leads to very severe wear rates on the rail especially under sanding conditions which have been reported as greatly increasing wear rates compared normal dry contacts [16].

The simulations have not included dry rail conditions which will produce much more severe surface fatigue index results than the modelled wet sanding. So whilst high adhesion locomotive operation can be expected to dramatically increase surface fatigue the wet rail simulation results suggest rail wear will dominate surface cracking except under AY-FS bogie.

Thermal damage to rail from wheel slide events is predicted from the simulation. The modelled simple traction control used in these simulations resulted in extended wheel slip. If such slips occurred in practice the flash temperatures would be sufficient for white etching layers to occur. The white etching layer in lab testing has shown accelerated RCF initiation and growth in wet conditions, [17].

CONCLUSION

The Cowan Bank with its combination of steep grades and tight curves is a severe test for the locomotive traction/train configurations under consideration. As such, this site presents challenges for the use of high adhesion locomotives.

There is a negative slope to the creep coefficient curve after creep saturation that is caused by temperature rise in the wheel rail contact. As a result of the negative slope the maximum adhesion at the wheel rail contact decreases with angle of attack. This can lead to uncontrolled wheel slip with further losses in adhesion performance. It is therefore important for driving wheelsets to maintain a low angle of attack and avoid lubricated or non sanded flange contact. The locomotives traction control and sanding equipments ability to raise wet rail adhesion has a major influence on adhesion.

Force steering bogies (which are still passive by definition) achieve partial steering with adhesion losses seen due to flanging on the end axles. The simulation shows adhesion losses of ~15 kN on the front locomotive and up to 40 kN for a third pulling locomotive for forced steered bogies on Cowan bank. Other passive bogies loose 30-70 kN tractive effort per locomotive. Hence the simulations of the passive steering bogies fail the high adhesion demands in wet conditions. The resulting high angles of attack induce uncontrolled wheel slip to occur and train failure.

Using the same simulation method and parameters, considerably better results were obtained with the AY-FS bogie, which included active steering control. The simulated AY-FS bogie was able to achieve the required adhesion on Cowan bank even with the relatively simple (and rough) traction control model used. These bogies are able to maintain low angles of attack to the rail and minimal flanging contact.

The AY-FS bogie has lower Tγ values reducing the risk of wheel slip and high wear rates but does not eliminate fatigue damage due to the high adhesion demand.

ACKNOWLEDGEMENTS

The authors acknowledge the assistance of RailCorp in providing background and case information for the study, the support of the Centre for Rail Engineering at CQU who have supported the work. The authors also acknowledge Desolver for support with vehicle dynamics simulation and the use of the GENSYS software in the study.

REFERENCES

1. Simson S, Cole C (2008), Simulation of curving at low speed under high traction for passive steering hauling locomotives, Vehicle System Dynamics, v 46, No.12 Nov 2008, pp 1107-1121, Taylor & Francis, UK.
2. Simson S, (2010), Three axle locomotive bogie steering, simulation of powered curving performance passive and active steering bogies, PhD thesis CQ University May 2010.
3. Simson S, Cole C (2009), Simulation of traction curving for active yaw – force steered bogies in locomotives, Rail & Rapid Transit, Part F – Proceedings institute of Mechanical Engineers, UK. Vol. 223, No. 1, 2009, pp 75-84.
4. Anon, Proposed Multiple AC drive locomotive running time test on the RailCorp network, RailCorp internal document
5. Ramsey N, Szanto F, Hewison P, Introducing the next generation locomotive to the Australian rail network, CORE2008 RTSA, pp 471-479
6. Cole C, Chapter 9 Longitudinal train dynamics, Handbook of railway vehicle dynamics, Ed. vIwnicki S, Taylor and Francis pp 239-278
7. Cole C, Simson S, Bosomworth C, Hayman M, McLeod T, Advances in in-cabin systems for the management of long trains, Proceedings of International Heavy Haul Conference 11th-13th June 2007, Lulea, Sweden. Lulea, Sweden IHHA Inc., 2007. p. 305-312
8. Ekberg A, Chapter 7 Fatigue of railway wheels, Wheel-rail Interface handbook Ed Lewis R & Olofsson, Woodhead Publishing 2009, pp 211-244.
9. Bohmer A, Ertz M, Knothe K, 2003, Shakedown limit of rail surfaces including material hardening and thermal stresses, Journal of Fatigue and Fracture Engineering of Material Structures Vol. 26, pp 985–998, Blackwell Publishing Ltd.
10. Tomberger C, Dietmaier P, Sextro W, Six K, Friction in wheel-rail contact: a model comprising interfacial fluids, surface roughness and temperature, Proceedings of the 8th International Conference on Contact Mechanics and Wear of Rail/Wheel systems, Firenze Italy, 2009
11. Ertz, M, Knothe K, A comparison of analytical and numerical methods for the calculation of temperatures in wheel/rail contact. Wear, (2002) 253(3-4) pp 498-508.
12. Polach O, Creep forces in simulations of traction vehicles running on adhesion limit, Wear (2005) 258 pp 992–1000
13. Polach O, Influence of locomotive tractive effort on the forces between wheel and rail, Vehicle Systems Dynamics (2001) Vol. 35 S1 pp 7–22
14. Burstow M, Whole life rail model application and development for RSSB – development of an RCF damage parameter. AEATR-ES-2003-832, Issue 1, Rail Safety & Standards Board, London, UK, October 2003, available from http://www.rssb.co.uk.
15. Eckberg A, Kabo E, Andersson H, An engineering model for prediction of rolling contact fatigue of railway wheels, Fatigue and fracture of engineering material structures 2002 Vol 25, pp 899-909
16. Fletcher D, Chapter 9 Rail surface fatigue and wear, Wheel-rail Interface handbook Ed Lewis R & Olofsson, Woodhead Publishing 2009, pp 280-310.
17. Carroll R, Benyon J, Fletcher D, Rolling contact fatigue of white etching layer, part 1, Wear 262 (2007) pp 1253-1266.